Investigations of the Synergy of Composite Cycle and Intercooled Recuperation

Sascha Kaiser, Markus Nickl
kaiser.sascha@gmail.com
Bauhaus Luftfahrt e.V.
Visionary Aircraft Concepts
82024 Taufkirchen
Germany

Christina Salpingidou, Zinon Vlahostergios
Aristotle University of Thessaloniki
Lab. of Fluid Mechanics and Turbomachinery
Thessaloniki
Greece

Stefan Donnerhack, Hermann Klingels
MTU Aero Engines AG
80995 München
Germany

ABSTRACT

The synergistic combination of two promising engine architectures for future aero engines is presented. The first is the Composite Cycle Engine, which introduces a piston system in the high pressure part of the core engine, to utilize closed volume combustion and high temperature capability due to instationary operation. The second is the Intercooled Recuperated engine that employs recuperators to utilize waste heat from the core engine exhaust, and intercooler to improve temperature levels for recuperation and to reduce compression work. Combinations of both architectures are presented and investigated for improvement potential with respect to specific fuel consumption, engine weight and fuel burn against a turbofan. The Composite Cycle alone provides a 15.6% fuel burn reduction against a turbofan. Options for adding intercooler were screened, and a benefit of up to 1.9% fuel burn could be shown for installation in front of piston system through a significant, efficiency-neutral weight decrease. Waste heat can be utilized by means of classic recuperation to the entire core mass flow before the combustor, or alternatively on the turbine cooling bleed or a piston engine bypass flow that is mixed again with the main flow before the combustor. As further permutation, waste heat can be recovered either after the low pressure turbine - with or without sequential combustion - or between the high pressure and low pressure turbine. Waste heat recovery after the low pressure turbine was found to be not easily feasible or tied to high fuel burn penalties due to unfavourable temperature levels, even when using sequential combustion or intercooling. Feasible temperature levels could be obtained with inter-turbine waste heat recovery, but always resulted in at least 0.3% higher fuel burn compared to the non-recuperated baseline under the given assumptions. Consequently, only the application of an intercooler appears to provide a considerable benefit for the examined thermodynamic conditions in the low fidelity analyses of various engine architecture combinations with the specific heat exchanger design. Since the obtained drawbacks of some waste heat utilization concepts are small, innovative waste heat management concepts coupled with the further extension of the design space and the inclusion of higher fidelity models may achieve a benefit and motivate future investigations.

Keywords: Composite Cycle; Recuperation; Intercooling; Propulsion; Novel Concepts

NOMENCLATURE

CCE	Composite Cycle Engine
HEX	Heat Exchanger
HPC	High Pressure Compressor
HPT	High Pressure Turbine
IC	Intercooler
IPC	Intermediate Pressure Compressor
IR	Intercooled Recuperation
LPT	Low Pressure Turbine
PC	Piston Compressor
PE	Piston Engine
PPS	Power Plant System
REC	Recuperator

Symbols

A	Heat exchanger area; m^2
BPR	Bypass Ratio
C	Heat capacity rate; W/K
c_p	Specific heat capacity; J/kg/K
FB	Fuel Burn
FHV	Fuel Heating Value; MJ/kg
k	Heat transfer coefficient; $W/m^2/K$
m	Mass; kg
M	Mach number
NTU	Number of Transfer Units
OPR	Overall Pressure Ratio = p_{35}/p_2
p	Total pressure; Pa
T	Total temperature; K
TSFC	Thrust Specific Fuel Consumption; g/kN/s
v	Velocity; m/s
w	Mass flow rate; kg/s
ε	Heat exchanger effectiveness
η	Efficiency

Subscripts

0	Free-stream
1-5	Engine stations (see Fig. 8)
c	Compressor
cold	Heat exchanger cold side
cool	Cooling flow
ex	Heat exchanger exit
in	Heat exchanger inlet
hot	Heat exchanger hot side
mat	Heat exchanger matrix
p	Polytropic
plumb	Heat exchanger plumbing
rel	Relative
t	Turbine

1.0   INTRODUCTION

Radical engine concepts are being investigated to improve engine efficiency beyond the limits of the Joule-/Brayton-cycle based turbofan engine to aim to achieve ACARE 2050 emission reduction targets [1,2]. These suggest a reduction of CO_2 emissions per passenger kilometre by 68% compared to year 2000 technology

standard coming from reduced energy demand by propulsion system and aircraft [2]. Assuming an equal contribution by both, the propulsion system would need to contribute a reduction of emissions by 43%. Alternatively, a part of the energy demand may be retrieved through installation effects reducing the required power to generate a given amount of thrust, such as boundary layer ingestion [3]. This may reduce the emissions by 7%, still requiring further 40% reduction by propulsion system and aircraft [4]. From today's perspective, it appears highly unlikely that such radical improvements can be achieved with the conventional Joule-/Brayton-cycle [5]. Under realistic assumptions, even the target of achieving a 30% emission reduction by a turbofan architecture appears to be very challenging [5]. For example, for a large turbofan with entry into service year 2025, an improvement of 23.4% was forecasted [6], and the Rolls-Royce UltraFan™ has a projected efficiency improvement of 25% with year 2025+ technology readiness [7]. Therefore, the investigation of novel architectures is warranted.

One promising candidate concept is the Composite Cycle Engine (CCE) that allows fuel burn improvements of 15-20% compared to a Joule-/Brayton-based turbofan of similar technology level. The CCE uses a highly charged piston based gas generator in the core engine, pressurized by turbo compressors, and turbines for power extraction. In this way, the CCE combines high efficiency and high peak temperature capability of piston engines and the high power density of turbomachinery. An example conceptual arrangement is depicted in Fig. 1 with a piston system placed between the combustor/turbine section of the core engine and the bypass duct. The piston system is charged by an intermediate pressure compressor and pre-cooled by an intercooler located directly upstream of the piston system. The piston system is mechanically decoupled from the turbo shafts to allow rotation at an independent speed and to dispense with the necessity for a gearing system.

Design considerations, engine configuration and off-design behaviour are discussed in reference [8]. It applied the concept to a regional aircraft platform with a regional turbofan of year 2025 technology standard with a crankshaft connected piston system, and showed a fuel burn advantage of 15.2% for the CCE. Further studies showed a consistent advantage of about 18% for both state of the art technology and year 2035 technology standard [5]. Challenges associated with the concept are engine weight increase of 17-32%, mainly driven by the piston components, and demanding operating conditions for the piston components at high temperatures and pressures.
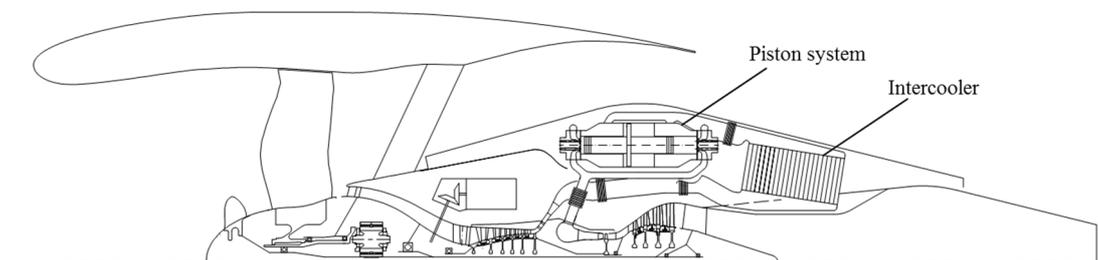

Fig. 1: Conceptual drawing of a Composite Cycle Engine with intercooler (adapted from [9]).

Another promising concept is Intercooled Recuperation (IR) in aero engines exploiting exhaust gas waste heat by utilizing it to preheat the intercooled compressor discharge air before it enters the combustion chamber resulting in reduction of fuel consumption and pollutant emissions. This concept is based on the integration and use of a number of heat exchangers, comprising a recuperator system, carefully mounted inside the hot gas exhaust nozzle, in order to avoid induced pressure losses, and an intercooler mounted between the compressor stages, so as to reduce the required compressor work. This concept has been mostly developed by MTU Aero Engines AG and investigated in large European funded research projects such as: CLEAN (Component vaLidator for Environmental-friendly Aero-eNgine), AEROHEX (Advanced Exhaust Gas Recuperator Technology for Aero-Engine Applications), NEW Aero engine Core concepts (NEWAC) and Low Emissions Core-Engine Technologies (LEMCOTEC) [10,11,12].

The intercooled recuperative engine concept is schematically shown in Fig. 2 and Fig. 3 together with the MTU developed state-of-the-art tubular heat exchanger (HEX) of elliptic tube profile.
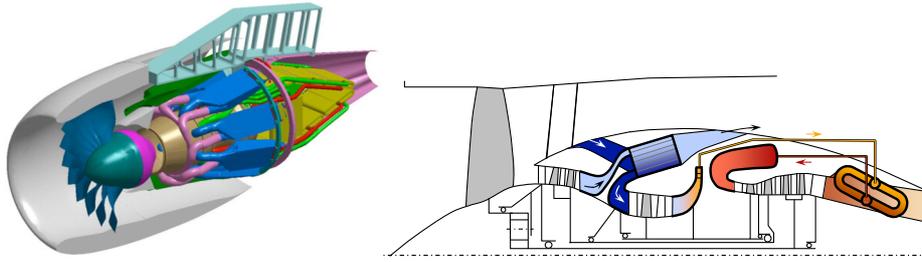
Fig. 2: The IR turbofan engine concept, developed by MTU Aero Engines [10].
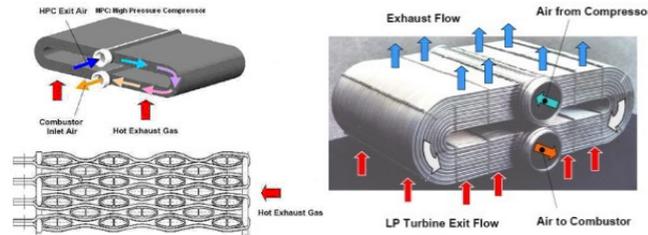

Fig. 3: The heat exchanger consisting the recuperator's installation [10].

In this paper, architectures for synergistic combinations of CCE and IR are explored and analysed through a conceptual analysis approach. The target of the studies is to identify thermodynamically feasible and beneficial generic configurations. At first sight, the introduction of heat exchanger addresses the challenges of the CCE and further improves fuel utilization. This may be achieved by Intercoolers (ICs) reducing the piston system's thermal load and weight, and/or Recuperators (RECs) utilizing waste heat to improving efficiency.

An IC may be introduced either between Intermediate Pressure Compressor (IPC) and Piston Compressor (PC), or between PC and Piston Engine (PE), as presented in Fig. 4. The first option in Figure 4(b) aims to reduce power required for compression in the PC and to reduce piston system size by increasing fluid density. The second option in Figure 4(c) allows to cool the air in front of the PE considerably in order to reduce thermal loads downstream the IC. This dispenses with power and weight saving in the PC and has a large penalty in thermal efficiency, because heat is removed at high pressure.
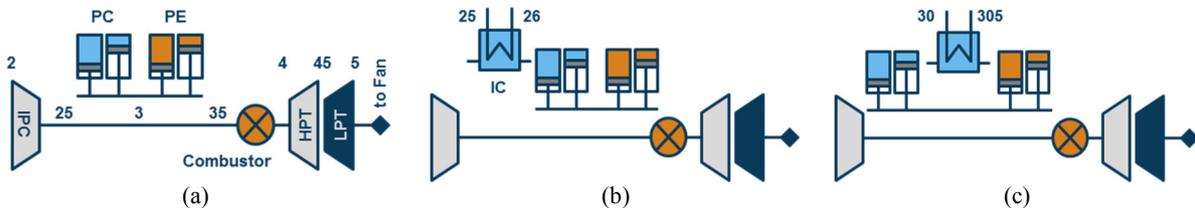

Fig. 4: Schematic drawings of (a) the baseline and (b,c) intercooler installation options with station nomenclature.

To recover waste heat for the purpose of reducing fuel consumption, several options are conceivable as displayed in Fig. 5. First, a heat exchanger may be employed as a classical REC after the LPT to transfer heat from the exhaust flow to the main flow after the piston system and before the combustor (Fig. 5 (a)), reducing fuel required. Second, the cooling air flow extracted after the PC may be preheated before being used in the HPT as proposed by [9] (Fig. 5 (b)). The cooling air has a lower temperature than the piston engine exhaust temperature at given cycle parameters. Furthermore, it operates on a small mass flow and reduces thermal gradients in the cooled HPT blades. On the flip side, cooling air mass flow ratio increases since the cooling air is preheated. Third, the REC may be supplied with air which bypasses the piston engine and is mixed with piston engine air before the combustor (Fig. 5 (c)). Here, the air also has a low temperature after the PC. The air used for recuperation is not available for the PE in addition to the cooling bleed mass flow. Adding heat before the PE appears promising thermodynamically, because the topping cycle would operate at even higher temperature levels. This option has been rejected, because piston engine size would increase, and the material constraints are already very challenging due to high temperatures in the piston cycle. Breakthrough material solutions for piston engines would warrant a revisitation of this kind of cycle, however.
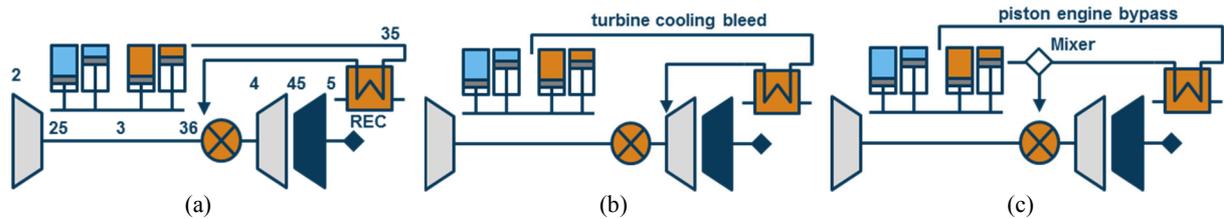
Fig. 5: Schematic drawings of heat exchanger application options: (a) Recuperator, (b) Bleed Pre-Heater, and (c) Bypass Recuperator with station nomenclature.

The temperature levels in a typical CCE cycle make achievement of recuperation after the LPT difficult, especially when the cycle parameters are optimized for optimal PE operation and when no additional modifications for the CCE are made. For example, the piston engine exhaust temperature T_{35} of the CCE baseline cycle used in this paper is 1190 K at top of climb, while the LPT exit temperature T_5 is only 700 K as displayed in Fig. 6. The resulting temperature difference is 490 K in the wrong direction, meaning recuperation is not feasible under these conditions.
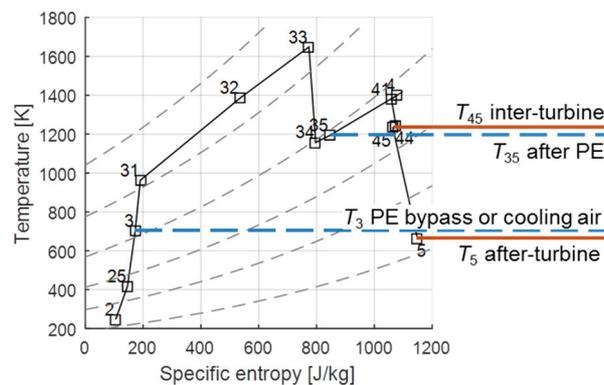

Fig. 6: Temperature over entropy diagram for the CCE baseline cycle with $T_4 = 1400$ K and OPR = 33. For useful heat exchange, the red, solid line must be over the blue, dashed line.

As a result, the CCE, IC and REC concepts have the potential to operate synergistically, if other conditions are chosen that imply a different power balance not specifically optimized for a CCE concept without IR, and provide an overall optimized cycle performance. Therefore, two additional modifications for improved waste heat management exploitation are investigated . First, sequential combustion may be employed between High Pressure Turbine (HPT) and Low Pressure Turbine (LPT) to raise the exhaust temperature level (Fig. 7(b)). The heat in the second combustor is added at low pressure, thus having a lower work potential. Second, the REC may be relocated between the HPT and the LPT (inter-turbine recuperation, Fig. 7(b)). This location clearly improves the temperature conditions for recuperation, but heat is extracted before the LPT, thus reducing the work potential. In both cases, the drawbacks would need to be over-compensated by recuperation.
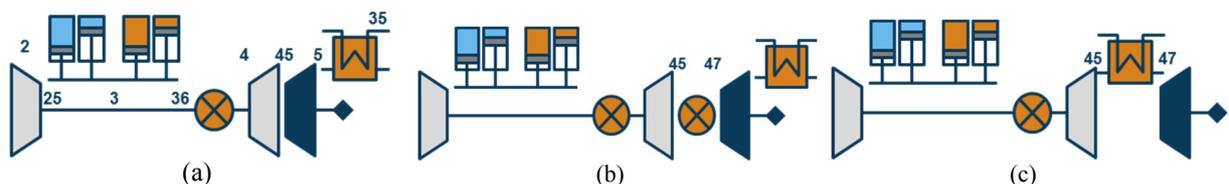

Fig. 7: Schematic drawings of heat exchanger installation location options: (a) After-turbine, (b) sequential combustion, and (c) inter-turbine with station nomenclature.

To examine the applicability of the heat exchanger options and combinations of them, they were benchmarked in parametric studies varying Overall Pressure Ratio (OPR) and combustor exit temperature T_4, and were assessed on a conceptual level. The ranges were chosen to also account for cycles with high T_4 and low OPR, which may enable temperature conditions allowing for recuperation. The modelling approach is introduced in the next section. From the parametric studies, the useful and feasible architectures combining CCE and IR were deducted in the 'Results' section. There, the concepts were evaluated using Thrust Specific Fuel Consumption (TSFC), engine weight and Fuel Burn (FB).

2.0   METHODS

The power plants are modelled in a simple and robust manner in order to allow quick implementation of novel architectures and validity of the results in a large range of parameters. The base architectures are set up as depicted in Fig. 8 combining inner fan, IPC and HPC into one unit, driven by the HPT. This simplifies calculation procedures and the definition of figures of merit, particularly core efficiency according to [13]. Thermodynamics are represented with half-ideal gas properties and chemical equilibrium combustion characteristics. The piston system is represented as a Seiliger cycle with adapted performance parameters. The detailed modelling is extensively described in [5]. The method set represents the most important design parameters by incorporating compressor sizing effects, cooling air demand and preliminarily component weights. The weight of the turbo components and piston components is estimated based on simple geometric representations, and were calibrated to state-of-the-art turbofan engines.
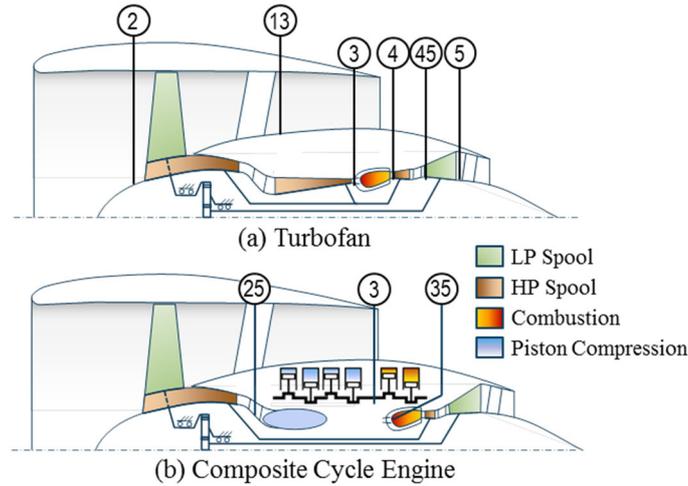

Fig. 8: Power plant schematics with station nomenclature (adapted from [5]).

The component efficiencies were adapted to reflect an improvement for the turbofan engine of 25% for year 2050 compared to year 2000 technology level. The assumptions are summarized in Table 1. It may be highlighted that turbo component efficiencies additionally include mechanical shaft, bearing and power gear box losses as well as customer power offtakes. The denoted combustion chamber pressure loss comprises losses in the combustion chamber itself, turbo compressor and turbine duct, and the core nozzle. For sequential combustion chamber, half of that loss, i.e. 3.75%, is assumed since it only represents the combustion chamber loss itself. The bypass pressure drop additionally includes stream tube, intake and bypass nozzle losses. Mechanical losses in the piston system were now accounted for as 4% of the work obtained during the PE expansion stroke, which corresponds to about 7.5% of the net output shaft power or a friction mean effective pressure of 70 kPa under design, top of climb conditions.

Table 1
Assumed technology standard for a year 2050 engine.

Variable	Unit	Value
General		
Fan efficiency $\eta_{p,fan}$	%	93.5
Compressor eff. $\eta_{p,c}$	%	92.0
Turbine eff. $\eta_{p,t}$	%	89.5
$\Delta p/p$ Combustion chamber	%	7.5
$\Delta p/p$ Bypass	%	2.5
Fuel Heating Value	MJ/kg	42.8
Specific bypass thrust	m/s	76
Composite Cycle Engine		
Piston compression eff.	%	95
Peak piston pressure	MPa	12
Mean piston velocity	m/s	22
Δp piston engine	kPa	100
PC pressure ratio	-	6.0

The engines are compared for an application to an intercontinental wide-body aircraft (design range 7000 nm, 300 passengers, cruise Mach number 0.80). A preliminary sizing thrust of 59.4 kN was assumed with a fan diameter of 3.50 m. The aerodynamic sizing point is at top of climb (35,000 ft, ISA, M0.8).

The parametric studies allow to conclude TSFC, basic geometric engine dimensions (such as fan diameter), and a simplified estimation of component weights. The impact on aircraft level in contrast to the reference turbofan can then be deducted with trade factors. These allow to calculate the change in fuel burn due to changes in TSFC and power plant system mass m_{PPS} including cascading effects due to changed aircraft weight and resizing of the aircraft structures. The trade factors are

$$\Delta FB_{TSFC} = 1.44 \cdot \Delta TSFC \qquad\qquad (\quad 1 \quad)$$

$$\Delta FB_m = 0.00238 \frac{\%}{\text{kg}} \cdot \Delta m \qquad\qquad (\quad 2 \quad)$$

based on the relative change in TSFC and the absolute change in mass. They were derived using an in-house aircraft simulation environment [14,15]. Other engine characteristics having a significant impact on aircraft performance are engine length, engine center of gravity. The first may increase nacelle and cowling drag. Also, longer shafts may incur problems with vibrations or buckling. The second may have adverse impact on wing torsional moment. These effects were not quantified, because they require a specific engine conceptualisation, which is not available at the level of detail of this study. These require close attention at further concept detailing. Impact on turbo component efficiency and compressor surge margin due to instationary boundary conditions to the piston components have been neglected, because previous studies indicated that the pressure amplitude can be reduced to a tolerable level.

A heat exchanger model has been added to simulate ICs and RECs, and adequately represent pressure drop and weight of heat exchanger matrix and plumbing. The models scale the heat exchanger according to heat exchanger effectiveness ε by means of Number of Transfer Units (NTU)

$$NTU = \frac{k \cdot A}{\min(C_{\text{hot}}, C_{\text{cold}})} \qquad\qquad (\quad 3 \quad)$$

with the heat transfer coefficient k, the heat exchange area A, and the minimum of the hot side and the cold side heat capacity rate C_{hot} and C_{cold}. The heat capacity rate C depends on the specific heat capacity c_p and the mass flow rate w

$$C = c_p \cdot w \qquad\qquad (\quad 4 \quad)$$

It is assumed that the ratio of heat capacities $C_{\text{hot}}/C_{\text{cold}}$ is one. The heat exchanger effectiveness ε is defined as

$$\varepsilon = \frac{T_{\text{cold,ex}} - T_{\text{cold,in}}}{T_{\text{hot,in}} - T_{\text{cold,in}}} \qquad\qquad (\quad 5 \quad)$$

with the cold side inlet and outlet temperatures $T_{\text{cold,in}}$ and $T_{\text{cold,ex}}$ as well as the hot side inlet temperature $T_{\text{hot,in}}$. The NTU for a cross-flow heat exchanger can then be related with ε according to [16] with the following fit valid between ε=0.3-0.8:

$$NTU = \frac{0.9 \cdot \varepsilon}{0.882 - \varepsilon} \qquad\qquad (\quad 6 \quad)$$

Choosing a heat capacity ratio $C_{\text{hot}}/C_{\text{cold}}$ other than one results in a higher heat exchanger effectiveness ε for a given NTU, but overall losses increase [17]. It may still be considered to achieve a more compact HEX or lower losses of one side on the HEX.

This approach including Eq. (6) presents a simplification to describe IC and REC behaviour for conceptual investigation. More dedicated and refined correlations that take variations of the heat capacity ratios into consideration must be adopted, in order to quantify the IC and REC beneficial contribution more accurately to the overall thermodynamic cycle. As can be seen from Eq. (3), heat exchanger area A and heat transfer coefficient k can be traded for a given NTU. With the target of a compact and lightweight design for aero engines, i.e. small A, the heat transfer k needs to be large. High heat transfer usually required high pressure drop across the heat exchanger Δp. Based on the above assumption, which will be further refined in future work, and assuming a constant heat transfer coefficient k and specific heat capacity c_p of the flow, the heat exchanger area

A is proportional to NTU and mass flow rate w. The matrix weight m_{mat} is assumed to be proportional to A. Calibrating the values for IC and REC to values given for $\varepsilon = 0.75$ in [16], the following matrix weights dependent on ε and w were derived:

$$m_{mat,IC} = 3.2 \cdot w_{IC} \cdot \frac{\varepsilon}{0.882 - \varepsilon} \qquad (\quad 7 \quad)$$

$$m_{mat,REC} = 9.0 \cdot w_{REC} \cdot \frac{\varepsilon}{0.882 - \varepsilon} \qquad (\quad 8 \quad)$$

The plumbing weights m_{plumb} are additionally considered according to [16] with

$$m_{plumb,REC} = 0.8 \cdot m_{mat,REC}(\varepsilon = 0.75) \qquad (\quad 9 \quad)$$

$$m_{plumb,IC} = 0.2 \cdot m_{mat,REC}(\varepsilon = 0.75) \qquad (\quad 10 \quad)$$

REC plumbing weight is four times the IC plumbing weight due to the long piping required to get air from combustion chamber to LPT exhaust and back. Since the heat transfer coefficient k is assumed constant, the according relative pressure drops across the heat exchanger Δp on hot and cold side are also assumed constant independent of ε. Even though these assumptions do not take into consideration the direct interaction of heat exchanger design parameters on both pressure losses and heat transfer and, thus, fail to capture high-fidelity design sensitivities, this assumption can initially serve well on a conceptual analysis on a low-fidelity level. The pressure drops are calibrated against data from higher fidelity methods and summarized in Table 2. It must be mentioned that the pressure drop values of Table 2, can be further optimized with the integration of innovative recuperator concepts in aero engines providing additional benefits and potential. The latter will be included in future investigations in order to properly refine the recuperator effect on the pressure losses and the aero engine thermodynamic cycle.

Table 2
Heat exchanger hot side and cold side pressure drops.

Pressure drop Δp [%]	Value
IC hot side	6.0
IC hot side duct	1.0
IC cold side	5.7
REC hot side	6.0
REC cold side duct	2.0
REC cold side	5.7

3.0   RESULTS

A reference turbofan and CCE have been set up first to serve as benchmarks for the following concepts. The design point was selected to provide best fuel burn while respecting component limits and providing enough margins for take-off and operability margins for part-load. As depicted in Fig. 9 (a), best TSFC is achieved at the fringe of the invalid cycles, i.e. when all fuel is burnt in the piston engine and none in the Joule combustion chamber. Power plant mass increases towards low OPR and T_4 (Fig. 9 (b)), but the negative fuel burn impact by the higher weight is superseded by the improvements due to TSFC (Fig. 9 (c)), which is typical for long range aircraft [18]. A maximum permissible Joule combustion chamber entry temperature T_{35} of 1200 K was assumed (indicated by thick blue, solid line), to respect material constraints of the combustion chamber, while providing 100 K margin for take-off. This constraint limits permissible OPR. Therefore, the design point (yellow square) for best fuel burn was selected at $T_4 = 1400$ K and OPR = 33. A lower T_4 was omitted in order to retain enough operability margin for part-load (cruise).

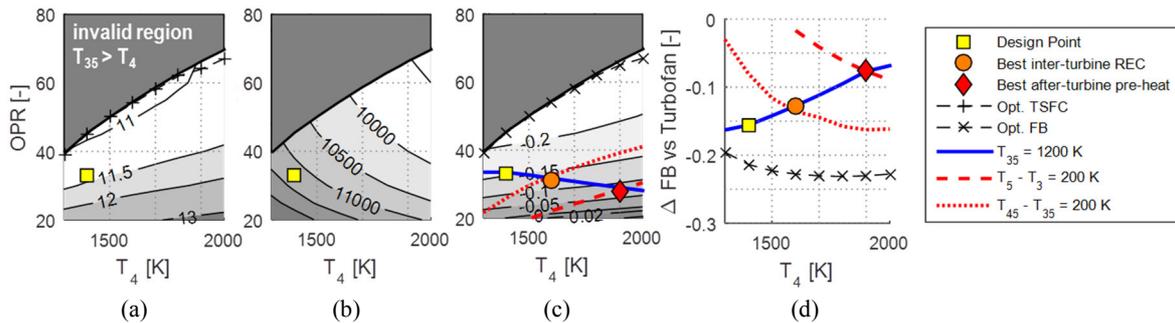(a)   (b)   (c)   (d)

Fig. 9: CCE parameter study results for (a) TSFC, (b) power plant system mass, and (c,d) fuel burn.

This design point offers a TSFC = 11.39 g/kN/s. For reference, the Joule-/Brayton-based engine has a TSFC = 13.14 g/kN/s. The main cycle properties are displayed in Table 3. It was assumed that the 25% turbofan TSFC improvement over year 2000 standard translates into a fuel burn improvement of 30% due to cascading effects. The CCE engine exhibits a 15.6% better fuel burn, but 20% higher power plant system weight than the year 2050 turbofan. The CCE requires a HPT relative cooling flow $w_{cool,rel}$ of only 5% as a consequence of the low OPR and T_4.

Table 3
Main engine properties of reference turbofan and CCE for year 2050.

Parameter	Turbofan	CCE
T_4 [K]	2000	1400
OPR [-]	75	33
TSFC [g/kN/s]	13.14	11.39
ΔFuel burn [%]	ref.	-15.6
ΔFuel burn vs. 2000	-30.0	-40.9
PPS mass [kg]	9340	11 220
BPR [-]	22.7	28.8
$w_{cool,rel}$ [%]	29.6	5.0

To allow a first reduction of the design space, targeted parameter combinations for recuperation and bleed pre-heating were investigated. For the respective studies, the heat exchanger was not yet implemented into the performance model, but the studies serve to identify whether there is merit to investigate the concepts in detail. For this purpose, a temperature difference of at least 200 K from hot side to cold side was stipulated for a beneficial heat exchange. This was set to achieve a notable heat flow and to overcome heat exchanger losses and weight. Also some margin must be provided for the reduced temperature levels during part-load (cruise). The 200 K limit may cancel out some feasible CCE and REC combinations. Additional analysis regarding this assumption will be made to future studies.

Below the thick red, dashed line in Fig. 9 (c,d) after-turbine bleed pre-heating and bypass recuperation is feasible (i.e. $T_3 < T_5$ - 200 K). It can be seen that the best parameter combination of OPR = 28 and T_4 = 1900 K (red diamond) has 8.0% higher fuel burn than the baseline CCE. Below the thick red, dotted line inter-turbine recuperation is feasible (i.e. $T_{35} < T_{45}$ - 200 K). Here, the best combination at OPR = 31 and T_4 = 1600 K (orange circle) has 2.8% higher fuel burn than the CCE. In both cases, the 200 K recuperation temperature delta would not to compensate the inferior cycle efficiency. An improvement that justifies the added complexity appears, therefore, unlikely with the given assumptions. At these two points, the heat exchanger operates at very challenging conditions (T_{45} = 1390 K). The application of an intercooler may alleviate this problem, which is discussed later in this paper. Classical recuperation (i.e. $T_{35} < T_5$ - 200 K) is never feasible within the parameter space even for high T_4 = 2000 K and low OPR = 20, while inter-turbine bleed pre-heating or PE bypass recuperation (i.e. $T_3 < T_{45}$ - 200 K) is always feasible. Therefore, the latter configurations will also be investigated in more detail later in the paper. A wider design space may be investigated to derive valid conclusions for all conceivable CCE and REC combinations.

Next, the application of ICs was investigated. The study in Fig. 10 shows fuel burn for the IC before the PC concept for varying heat exchanger effectiveness ε_{IC}. The results are summarized in Table 4. They clearly showcase the advantages of reducing piston system weight and fuel burn at the same time. Optimum intercooler effectiveness ε_{IC} is at about 70% with a fuel burn improvement of 17.5%, giving another 2.2% over the baseline CCE. The improvements clearly emerge from the reduced piston system weight, since the TSFC increases slightly over the CCE baseline (11.39 g/kN/s). Despite the additional IC weight of 320 kg, the total power plant system weight reduces by 1530 kg, or 13.6%. As an important finding, the OPR for optimum fuel burn increases considerably with increasing ε_{IC}, and T_4 increases moderately up to 1600 K for ε_{IC} = 0.7. This trend counteracts the cooling effort by the IC as the design point shifts towards the T_{35} constraint limiting combustion chamber inlet temperature to 1200 K. This induces the remarkable finding that as recuperation potential improves for given cycle parameters - as can be seen by the red lines shifting towards higher OPR (Fig. 10) - the optimum design point moves to higher OPR likewise.
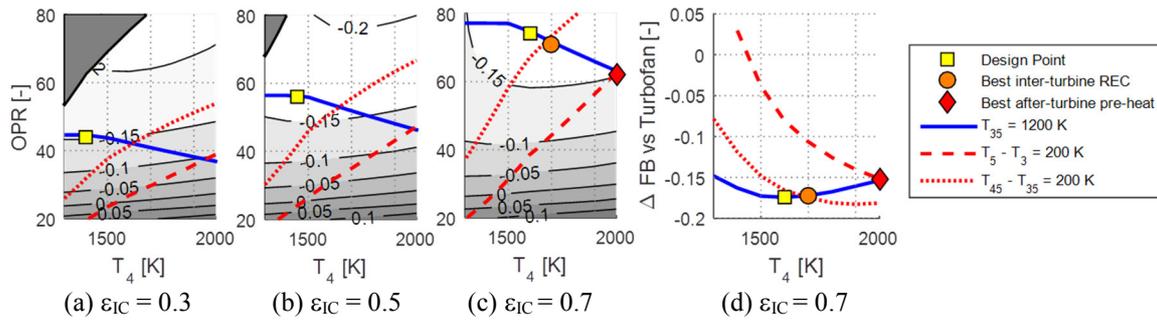
(a) $\varepsilon_{IC} = 0.3$ (b) $\varepsilon_{IC} = 0.5$ (c) $\varepsilon_{IC} = 0.7$ (d) $\varepsilon_{IC} = 0.7$

Fig. 10: (a-c) Fuel burn parameter studies for CCE with IC before PC for various ε_{IC} from 0.3 to 0.7, and (d) fuel burn comparison for $\varepsilon_{IC} = 0.7$.

Table 4

Main results of CCE with IC before PC for various ε_{IC}.

Parameter	Value		
ε_{IC}	0.3	0.5	0.7
T_4 [K]	1400	1450	1600
OPR	44	56	74
TSFC [g/kN/s]	11.45	11.43	11.48
ΔFuel burn [%]	-15.3	-16.9	-17.5
PPS mass [kg]	10 940	10 300	9 690
IC gross mass [kg]	200	200	320
BPR	28.8	30.9	36.0
$w_{cool,rel}$ [%]	5.0	5.2	6.9

The best parametric combination for bleed pre-heating (thick red dashed line) can be found at $\varepsilon_{IC} = 0.7$, $T_4 = 2000$ K, OPR = 62, and already has a 2.4% fuel burn penalty against the design point conditions. Additionally, adding heat to the flow before the combustion chamber would require to lower OPR in order to maintain a $T_{35} = 1200$ K constraint. Therefore, bleed pre-heating with after-turbine HEX was not studied further.

The best inter-turbine recuperation concept comes close to the design point of the non-recuperated cycle for $\varepsilon_{IC} = 0.7$, $T_4 = 1700$ K, OPR = 71, with a fuel burn penalty of only 0.3% against the design point fuel burn, but exhibits extremely high HEX temperatures. The hot side inlet temperature at this point is 1390 K with a pressure difference of 1.2 MPa to the cold side, rendering very challenging HEX operating conditions. Additionally, the OPR would need to be decreased when recuperating heat to the flow before the combustion chamber in order to maintain the $T_{35} = 1200$ K constraint, which further diminishes the improvement potential. Since no significant improvements can be expected with the selected assumptions justifying the added complexity, inter-turbine recuperation was not further investigated in this paper as well.

The results for the IC after the PC revealed that about the same weight savings can be achieved as for the IC before PC concept. The expected benefit of reduced piston engine system weight could be achieved with reduction of weight from 2390 kg (baseline) down to 1430 kg ($\varepsilon_{IC} = 0.5$). However, TSFC increases considerably to 12.11 g/kN/s ($\varepsilon_{IC} = 0.3$), and 12.46 g/kN/s ($\varepsilon_{IC} = 0.5$), resulting in an increase in fuel burn of 6.8% and 9.5% over the baseline CCE, respectively. Also, recuperation potential is not improved under the selected conditions and assumptions of the current study. Therefore, the second intercooler concept was disregarded for this paper.

When evaluating sequential combustion, the exit temperatures of both combustion chambers were set equal in the first instance. The resulting fuel burn is 4.2% worse than the baseline CCE. While the OPR for regions of feasible bleed pre-heating and bypass recuperation shifts upwards, the difference is not sufficient to enable it at the design point. The respective power plant system weight reduces by only 350 kg through increased core specific work.

Additional side studies were conducted to investigate the impact of the second combustion chamber temperature. A higher temperature results in even worse TSFC. A lower temperature leads to better TSFC with an optimum when fuel flow in the second combustor becomes zero, i.e. sequential combustion is removed.

Combining sequential combustion with IC showed the same trends with increased fuel burn of 3.8% ($\varepsilon_{IC} = 0.3$), 3.5% ($\varepsilon_{IC} = 0.5$), as well as 2.6% ($\varepsilon_{IC} = 0.7$), and only a small advantage in power plant system mass. Therefore,

sequential combustion cannot be used to improve fuel burn or to enable recuperation for concepts that did not feature feasible recuperation scenarios without sequential combustion.

As supplementary study, the PC pressure ratio was investigated as a design parameter to improve recuperation potential. Reducing PC pressure ratio results in reduced power demand from the PE, allowing a lower PE fuel flow and, hence, exit temperature T_{35}. Since the power balance now shifts from the efficient piston combustion to the constant pressure Joule combustor, core efficiency reduces at given OPR. On the flip side, OPR can be increased to approach the T_{35} constraint to remedy this effect. Ultimately, both effects cancel each other, providing no notable difference in fuel burn or recuperation potential.

To conclude the cursory studies, only inter-turbine bleed pre-heating and inter-turbine piston bypass recuperation allow for correct heat transfer with the potential for fuel burn improvement, and are therefore investigated closely in the following. Both concepts were also combined with an IC before the PC. Since both exchange heat to a relatively small mass flow compared to the main mass flow rate, compact heat exchangers with a low interference with the main flow may be employed. Therefore, it was assumed that the heat exchangers can be incorporated into the inter-turbine casing struts and the LPT stators, and the recuperator pressure loss on the hot side was optimistically set zero. Moreover, no penalty on inter-turbine duct pressure loss or LPT efficiency was assumed due to the additional heat exchangers. Therefore, the numbers serve to identify an upper bound for the efficiency potential.

The first option, inter-turbine bleed pre-heating, results in increased fuel burn as shown in Table 5. Without IC, TSFC increases slightly with rising bleed-preheater effectiveness ε_{REC}. Although heat is recovered from the turbine exhaust, relative cooling flow must increase considerably to account for the rising cooling air temperature. PPS mass increases due to rising core mass flow, increasing fuel burn by 0.6% ($\varepsilon_{REC} = 0.3$) and 2.0% ($\varepsilon_{REC} = 0.5$). Adding an IC, the detrimental impact can be reduced as seen in Table 5. With an IC effectiveness $\varepsilon_{IC} = 0.5$ and $\varepsilon_{REC} = 0.5$, the cooling mass flow $w_{cool,rel}$ increases to 11.6% instead of 13.6% without IC, but the fuel burn is still 1.4% higher than with intercooling only. Hence, adding a cooling bleed pre-heater cannot be used to improve fuel burn or engine weight.

Table 5
Cycle results for inter-turbine bleed pre-heating.

Parameter	Value			
	Non-intercooled		**Intercooled ε_{IC}=0.5**	
ε_{REC}	0.3	0.5	0.3	0.5
T_4 [K]	1400	1400	1400	1400
OPR [-]	32	30	54	52
TSFC [g/kN/s]	11.41	11.49	11.45	11.48
ΔFuel burn [%]	-15.0	-13.6	-16.1	-15.5
PPS mass [kg]	11 400	11 600	10 560	10 690
IC gross mass [kg]	-	-	220	230
REC gross mass [kg]	70	110	60	90
BPR	27.7	26.7	28.6	27.7
$w_{cool,rel}$ [%]	9.9	13.6	7.9	11.6

The second option, inter-turbine bypass recuperation, also results in higher fuel burn (Table 6). Since heat is recuperated before the combustion chamber, the OPR needs to be decreased in order to obey the T_{35} constraint. For $\varepsilon_{REC} = 0.5$, fuel burn increases by 1.0% when using 10% of the core mass flow as bypass air, and by 2.0% when using 20%. The effects aggravate when increasing ε_{REC}. Although the disadvantage is small, it does not justify the complexity of the heat exchanger and mixer which is added to the already increased complexity of the CCE cycle configuration. Moreover, the recuperator would need to operate at a hot side inlet temperature of 1240 K. The power plant system mass stays roughly constant. Adding an IC does not improve the results, and fuel burn increases by 0.4-1.4% for various combinations of $\varepsilon_{IC} = 0.3$-0.5 and $\varepsilon_{REC} = 0.3$-0.5 compared to the intercooled, non-recuperated engine.

Table 6
Cycle results for inter-turbine bypass recuperation with $\varepsilon_{REC} = 0.5$.
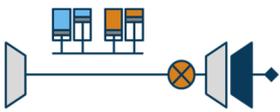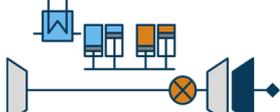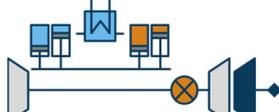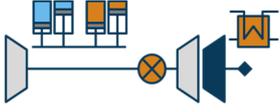
Parameter	Value			
	Non-intercooled		**Intercooled ε_{IC}=0.5**	
w_{bypass}/w_{25} [%]	10	20	10	20
T_4 [K]	1400	1400	1400	1400

OPR	31	29	52	49
TSFC [g/kN/s]	11.45	11.52	11.46	11.49
ΔFuel burn [%]	-14.6	-13.6	-16.1	-15.5
PPS mass [kg]	11 340	11 470	10 540	10 650
IC gross mass [kg]	-	-	220	230
REC gross mass [kg]	80	160	80	160
BPR	27.9	27.0	28.5	27.7
$w_{cool,rel}$ [%]	5.0	5.1	5.0	5.0

4.0 CONCLUSION

Various combinations of the Composite Cycle Engine concept with intercoolers, recuperators, and bleed pre-heaters were conducted. It was investigated whether heat transfer is feasible for various combinations of cycle parameters. Cycles allowing for positive heat transfer and showing a potential for fuel burn improvement over the base Composite Cycle Engine without heat exchangers were investigated further. The findings are summarized in Table 7. Further details are enlisted in Table A.1. The highest benefit can be achieved when using an intercooler before the piston compressor with a fuel burn improvement of 1.9% over the base cycle at intercooler effectiveness $\varepsilon_{IC} = 0.7$ (corresponding to a 42.2% improvement against year 2000), and a simultaneous power plant system weight reduction of 13.6%.

Table 7
Summary of findings for synergetic combination of Composite Cycle Engine with Intercooled Recuperation; all deltas relative to ref. Turbofan.

Non-recuperated			
numbers: Δfuel burn / Δweight vs. turbofan; all values at heat exchanger eff. ε=0.5			
	-15.6% / +20.1% <u>baseline</u>	-16.9% / +10.3% <u>intercooled baseline</u>: fuel burn and weight better than baseline	-6.1% / +6.3% considerably worse fuel burn than baseline (concept disregarded)

Recuperated, non-intercooled			
REC location / **Heat receiving fluid**			
Main flow after piston engine	Not feasible in entire parametric space	only feasible for cycles with >2.8% higher fuel burn and high heat exchanger temperature	Not feasible in entire parametric space
Turbine cooling bleed	only feasible for cycles with >8.0% higher fuel burn than baseline	-13.6% / +24.4% worse fuel burn and weight than baseline	Efficiency of baseline cycle decreases by 4.2%. Although feasible cycle parameter combinations get closer to baseline design point, the resulting fuel burn is >10.4% higher.
Piston engine bypass		-13.6% / +22.8% at 20% bypass mass flow; worse fuel burn and weight than baseline	

Recuperated, intercooled before piston compressor			
REC location / **Heat receiving fluid**			

Main flow after piston engine	Not feasible in entire parametric space	only feasible for cycles with >0.3% higher fuel burn and high heat exchanger temperature	Not feasible in entire parametric space
Turbine cooling bleed	only feasible for cycles with >2.4% higher fuel burn than intercooled baseline	-15.5% / +14.5% worse fuel burn and weight than intercooled baseline	Efficiency of baseline cycle decreases by 3.5%. Although feasible cycle parameter combinations get closer to baseline design point, the resulting fuel burn is >6.6% higher.
Piston engine bypass		-15.5% / +14.0% at 20% bypass mass flow; worse fuel burn and weight than intercooled baseline	

Temperature levels after the low pressure turbine are generally too low to allow for heat recovery to the flow after the piston engine. For recuperation to the flow before the piston engine, the parametric combinations of Overall Pressure Ratio and combustor exit temperature allowing for it are far from the optimum cycle combinations, rendering a beneficial application unfeasible. Inter-turbine recuperation to the core flow after the piston engine was also excluded due to a very marginal recuperation potential at very challenging conditions for the recuperator at peak temperatures over 1300 K. This conclusion is guided by the assumptions used for the current parametric investigations. Additional studies to a more extended design space and also including other HEX architectures are necessary in order to derive an accurate overall conclusion regarding the various synergy potentials.

Only inter-turbine recuperation to the flow before the piston engine showed reasonable recuperation potential and was evaluated quantitatively. Even with optimistic assumptions, the studies showed that pre-heating the turbine cooling bleed increases core mass flow and TSFC, resulting in increased fuel burn. The drawbacks of recuperation to piston bypass are smaller, but still no improvement in TSFC, engine mass or fuel burn could be obtained. Hence, the inclusion of the additional complication of recuperation is not justified.

To conclude, the application of intercoolers shows significant potential for fuel burn improvement and may be investigated in greater detail in conceptual studies. Challenges going forward are the conceptual arrangement of the technology into the limited core engine space. Operational characteristics need to be investigated to assess, whether the benefits persist in part load conditions. Otherwise, a variable flow path may be required that allows bypassing the intercooler during part load operation. Moreover, the impact on take-off performance needs to be verified when intercooling is employed.

Detailed analysis of material options, piston cooling technology and piston engine performance must be made in order to evaluate the real conceptual benefits of pre-cooling the piston system. Some synergetic combinations of the Composite Cycle Engine and Intercooled Recuperation were excluded with the presented assumptions, because they showed small disadvantages in fuel burn and engine weight, while operating at challenging conditions and increasing engine complexity. It is needless to say that innovative heat exchanger concepts or leaps in heat exchanger technology may turn the impact on overall engine level into an advantage. In that case, these architectures should be revisited. Generally it was shown that high temperature heat exchangers are necessary to apply recuperation to meaningful cycle conditions.

ACKNOWLEDGMENTS

REFERENCES

[1]   "Flightpath 2050: Europe's Vision for Aviation", Publications Office of the European Union, Luxembourg, 2011, p. 15. doi:10.2777/50266

[2]   "Realising Europe's Vision for Aviation—Strategic Research and Innovation Agenda—Volume 1," Advisory Council for Aviation Research and Innovation in Europe (ACARE), Brussels, Belgium, Sept. 2012, pp. 145–147.

[3]   J. BIJEWITZ, A. SEITZ, A.T. ISIKVEREN, M. HORNUNG, "Progress in Optimizing the Propulsive Fuselage Aircraft Concept", AIAA-2016-0767, AIAA Science and Technology Forum and Exposition 2016, San Diego, CA, 2016.

[4]   T. GRÖNSTEDT, C. XISTO, O. SCHMITZ, S. DONNERHACK, A. LUNDBLADH, K. YAKINTHOS, A. SEITZ, V. SETHI, A. ROLT, P. NEWTON, N. TANTOT, N. GARCIA ROSA, "Ultra Low Emission Technology Innovations for Mid-Century Aircraft Turbine Engines", ASME Turbo Expo 2016, GT2016-56123, Seoul, South Korea, June 2016.

[5]   S. KAISER, A. SEITZ, P.C. VRATNY, M. HORNUNG, "Unified Thermodynamic Evaluation of Radical Aero Engine Cycles", ASME Turbo Expo 2016, GT2016 -56313, Seoul, South Korea, June 2016.

[6]   R. VON DER BANK, S. DONNERHACK, W. STURM, M. FLOUROS, D. BRUNA, M. STOKES, F. POUTRIQUET, S. BOURGOIS, T. OBRECHT, N. TANTOT, A. LUNDBLADH, F. WALLIN, S. FORSMAN, R. AVELLAN, A. ANTORANZ, O. CABALLERO, D. TORRE, M. MORALES, A. ORNAT, T. MRUGALA, L. KRAJ, A. PESCHIULLI, F. TURRINI, S. COLANTUONI, E. BASSET, Z. PALAT, M. RUZICKA, E. JOHANN, D. SEITZ, G. GEBEL, T. DÖRR, "Advances in Ultra-High Pressure Ratio Core Engines", 65. Deutscher Luft- und Raumfahrtkongress, DLRK2016-420006, Braunschweig, Germany, September 2016.

[7]   F. HASELBACH, A. NEWBY, R. PARKER, "Concepts & Technologies for the next Generation of Large Civil Aircraft Engines", 29th Congress of the International Council of the Aeronautical Sciences, St. Petersburg, Russia, September 2014.

[8]   S. KAISER, S. DONNERHACK, A. LUNDBLADH, A. SEITZ, "Composite Cycle Engine Concept with Hectopressure Ratio", Journal of Propulsion and Power, Vol. 32, No. 6, 2016. doi: 10.2514/1.B35976

[9]   H. KLINGELS, "Wärmekraftmaschine für Freikolbenverdichter", European Patent EP2650510 A2, 2013.

[10]   A. GOULAS, S. DONNERHACK, M. FLOUROS, D. MISIRLIS, Z. VLAHOSTERGIOS, K. YAKINTHOS, "Thermodynamics Cycle Analysis, Pressure Loss, and Heat Transfer Assessment of a Recuperative System for Aero-Engines", GTP-14-1470, J. Eng. Gas Turbines Power, Vol. 137, No. 4, 2015.

[11]   K. YAKINTHOS, D. MISIRLIS, Z. VLAHOSTERGIOS, M. FLOUROS, S. DONNERHACK, A. GOULAS, "Best Strategies for the Development of a Holistic Porosity Model of a Heat Exchanger for Aero Engine Applications", GT2015-42408, Proceedings of ASME Turbo Expo 2015: Power for Land, Sea and Air GT2015, Montreal, Canada, June 2015.

[12]   S. BOGGIA, K. RÜD, "Intercooled recuperated aero engine", Proceedings of the Deutscher Luft- und Raumfahrtkongress 2004, DGLR-2004-179, DGLR, Bonn, pp. 371-380, 2004.

[13]   J. KURZKE, "GasTurb 11 - Design and Off-Design Performance of Gas Turbines", Germany, 2007.

[14]   P. HEINEMANN, P. PANAGIOTOU, P. C. VRATNY, S. KAISER, M. HORNUNG, K. YAKINTHOS, "Advanced Tube and Wing Aircraft for Year 2050 Timeframe", AIAA Science and Technology Forum and Exposition, Grapevine, Texas, Jan. 2017. (abstract accepted)

[15]   "PACE - Pacelab APD", Pace GmbH, 2011.

[16]   H. GRIEB, "Projektierung von Turboflugtriebwerken", 1st Ed., Birkhäuser, Basel, 2004.

[17]   J.E. HESSELGREAVES, "Compact Heat Exchangers", Elsevier Science & Technology Books, Kidlington, Oxford, UK, 2001.

[18]   H. GRIEB, B. SIMON, "Pollutant emissions of existing and future engines for commercial aircrafts", Lecture Notes in Engineering, Vol. 60, *Air Traffic and the Environment - Background, Tendencies and Potential Global Atmospheric Effects*, Springer-Verlag Berlin Heidelberg, 1990, pp. 43-83. doi: 10.1007/978-3-642-51686-3

APPENDIX

Table A.1
Summary of important results for simulated engines.

	Turbofan	CCE Baseline	Best inter-turbine REC	Best after-turbine bypass REC	CCE IC Fig. 4(b)	Best IC inter-turbine REC	Best IC after-turbine bypass REC	CCE IC Fig. 4(c)	CCE inter-turbine bleed pre-heating	CCE IC inter-turbine bleed pre-heating	CCE Sequential Combustion	CCE inter-turbine bypass REC
T_4 [K]	2000	1400	1600	1900	1400 / 1450	1700	2000	1500 / 1600	1400 / 1400	1400 / 1400	1400 / 1450	1400 / 1400
OPR	75	33	31	28	44 / 56	71	62	43 / 50	32 / 30	54 / 52	33 / 56	39 / 49
ε_{IC} [%]	-	-	-	-	30% / 50%	70%	70%	30% / 50%	- / -	50% / 50%	- / 50%	30% / 50%
ε_{REC} [%]	-	-	-	-	- / -	-	-	- / -	30% / 50%	30% / 50%	- / -	50% / 50%
TSFC [g/kN/s]	13.14	11.39	11.7	12.22	11.45 / 11.43	11.52	11.74	12.11 / 12.46	11.41 / 11.49	11.45 / 11.48	11.81 / 11.80	11.54 / 11.49
ΔFuel burn vs. Turbofan [%]	ref.	-15.6%	-12.8%	-7.6%	-15.3% / -16.9%	-17.2%	-15.1%	-8.8% / -6.1%	-15% / -13.6%	-16.1% / -15.5%	-11.4% / -13.4%	-13.9% / -15.5%
PPS mass [kg]	9340	11220	10820	10480	10940 / 10300	9590	9410	10530 / 9930	11400 / 11600	10560 / 10690	10870 / 9950	11160 / 10650
IC/REC mass [kg]	3100	0	0	0	200 / 200	310	270	180 / 170	70 / 110	270 / 320	0 / 170	370 / 380
BPR	22.7	28.8	33.2	38.7	28.8 / 30.9	38.3	44.4	32.7 / 37	27.7 / 26.7	28.6 / 27.7	33.1 / 37.5	27.2 / 27.7
$w_{cool,rel}$ [%]	29.6%	4.9%	10.5%	18.6%	5% / 5.2%	10.2%	18.4%	5% / 5.5%	9.9% / 13.6%	7.9% / 11.6%	5.2% / 5.6%	5% / 5%
w_{bypass}/w_{25} [%]	-	-	-	-	- / -	-	-	- / -	- / -	- / -	- / -	20% / 20%